# Interatomic Potentials and Defect Energetics in Dilute Alloys

Abstract: Effective interatomic potentials for impurities in aluminum have been constructed according to pseudopotential theory. Based on a local model potential, impurity valence and size factors are defined and their effects on the potential discussed. With these potentials, detailed calculations based on a Green's function lattice statics method are made for the impurity-vacancy binding energy and the difference in diffusion activation energies for an impurity and a host atom.

Within the range of valence and size factors studied, it is found that the binding energy is generally small and depends primarily on the valence rather than the size, whereas the migration energy shows larger increases with both valence and size factors. Contributions from the lattice relaxation energies are important, particularly for impurity migration. The results can account satisfactorily for the experimental data of nontransition-metal impurities, but less so for the noble-metal impurities. Dielectric screening of the ion by the conduction electrons is important in determining the potential and must be properly accounted for in calculations of the energetics for impurities.

#### Introduction

Atomic diffusion in dilute alloys is strongly influenced by the nature of the interaction between vacancies and solute atoms. This diffusion plays an important role in many solid state phenomena. The formation of precipitates that contribute to alloy strengthening is one example having considerable practical importance. The phenomenon of impurity segregation to grain boundaries and voids is another example. It is, therefore, of some interest to obtain a quantitative understanding of the vacancy-impurity interaction. The physical parameters of primary interest in this regard are the binding energy for vacancy-solute pairs and jump frequencies for vacancy migration in the vicinity of a solute atom.

The purpose of the present paper is to develop an approach for the calculation of these parameters and to apply it to impurity diffusion in aluminum, for which extensive experimental data are available. Such calculations require 1) interatomic potentials describing the host-host and host-impurity interactions and 2) a procedure for including the effect of the lattice relaxation surrounding the point-defect configurations. An impurity is commonly characterized by its valence and "size". We have, therefore, attempted to vary these parameters in a systematic way to determine their effects on the energetics of the vacancy-impurity interaction.

This paper is divided into two parts. The first describes the construction of the interatomic potential within the framework of pseudopotential theory. Based on a local model potential, size and valence factors are

defined and their effect on the pair potentials discussed. The second part deals with the calculation of the impurity-vacancy binding energy and the difference in diffusion activation energies for an impurity and a host atom. Here, considerable effort has been spent in the calculation of lattice relaxation energies. For this purpose the Green's function formulation of lattice statics [1] has been used. The results, particularly for migration energies, show that lattice relaxation has a large effect.

Nontransition-metal impurities in aluminum were chosen as the subject of numerical calculations. This choice was motivated by the validity of the pseudopotential approach for aluminum and also the existence of some recent data for impurity diffusion and vacancy-solute binding energies [2]. For simplicity, we limit our study to nontransition-metal impurities. The transition-metal impurities, which have been found to have quite different diffusion behavior in aluminum, should be an interesting subject for future study.

# Interatomic potentials

Interatomic potentials for aluminum alloys are developed here within the framework of pseudopotential theory. Previously, vacancy-impurity interactions have often been studied according to interatomic potentials calculated from the Fermi-Thomas [3] screening potential or the asymptotic Friedel potential [4]. Recent reviews on the early models and their later refinements can be found in [2]. These models have been used recently [5],

but without much success, in attempts to explain the impurity diffusion data in aluminum. While the validity of the pseudopotential approach to describe lattice defects has not been rigorously established [6], this approach does represent a more serious attempt at a realistic theory than those used in previous work. Pseudopotential theory has at least two advantages over the above mentioned models: it avoids the nonrealistic pointion model, and it includes, at least approximately, the effect of electron gas exchange and correlation on the screening.

In this section the pseudopotential formulation of interatomic potentials is reviewed, and a discussion of the local model potential used in numerical calculations is given.

Consider a simple metal characterized by a nearly free-electron valence band. Its total energy can be divided according to pseudopotential theory into volume-dependent and structure-dependent parts [7]. The former includes the kinetic, exchange and correlation energies for a uniform electron gas plus the first-order correction from the electron-ion interaction. This part can be written as a function of the average electron density and is essential for maintaining the lattice equilibrium. The second part depends on the detailed atomic arrangement. It consists of the direct electrostatic interaction between ions, and the indirect ion-ion interaction through the screening of the conduction electrons. The latter is called the band structure energy and for pure metals can be expressed as [8]

$$U_{\rm BS} = N/2\Omega \sum_{k \neq 0} (k^2/2\pi) |V_{\rm i}(k)|^2 S(k) \left[ \left( \frac{1}{\varepsilon_k} \right) - 1 \right],$$

where  $\Omega$  is the atomic volume, N is the total number of ions,  $V_i(k)$ , called the strength function by Shaw [9], is the Fourier transform of the bare model potential of the ion, S(k) is the structure factor,  $\varepsilon_k$  is the dielectric function, and the sum extends over all reciprocal lattice vectors. Combining the ion-ion coulomb potential with  $U_{\rm BS}$  one can express the structure-dependent energy in terms of an effective potential  $\phi(r)$  given by [8]

$$\phi(r) = \frac{Z_{i}^{2} e^{2}}{r} \left[ 1 - \frac{2}{\pi^{2}} \int_{0}^{\infty} \frac{\left[ k^{2} V_{i}(k) \right]^{2}}{4\pi Z_{i} e^{2}} \left( \frac{1}{\varepsilon_{k}} - 1 \right) \frac{\sin kr}{k} dk \right].$$

A similar derivation can be carried out for a dilute alloy, and one arrives at an effective potential between "a" and "b" ions of the form [8]

$$\begin{split} \phi_{ab}(r) &= \frac{Z_a Z_b e^2}{r} \left[ 1 - \frac{2}{\pi^2} \int_0^\infty \left( \frac{k^2 V_a(k)}{4\pi Z_a e^2} \right) \left( \frac{k^2 V_b(k)}{4\pi Z_b e^2} \right) \right. \\ &\quad \times \left( \frac{1}{\varepsilon_b} - 1 \right) \frac{\sin kr}{k} \, dk \, \bigg], \end{split} \tag{1}$$

where the subscripts a and b refer to the two types of ions. In the dilute limit  $\varepsilon_k$  is simply the dielectric function for the pure host metal.

The separation of the total crystal energy into volumeand structure-dependent parts is very convenient for defect calculations in metals. In fact the parameters which we wish to calculate, i.e., binding energies and migration energies, may be expressed in terms of structural energies alone, as is shown in the appendix. In the calculation described in third and fourth sections, we require the pair potentials  $\phi_{aa}(r)$  and  $\phi_{ab}(r)$ . The remainder of this section is concerned with the determination of these quantities and particularly with the dependence of  $\phi_{ab}(r)$  on the size and valence of the impurity.

To construct the interatomic potentials, we require the explicit form of the pseudopotential for the host and impurity ions. As in previous work [10] we adopt a local potential having a simplified Heine-Abarenkov [11] form:

$$V_{i}(r) = \begin{cases} -V_{i} & r < R_{m}^{i} \\ \frac{-Z_{i}e^{2}}{r} & r > R_{m}^{i}. \end{cases}$$

Here i stands for either an impurity or a host atom. This model potential contains two parameters:  $V_i$ , the potential well depth and  $R_{\rm m}^{\ \ i}$ , the model radius of the ion. The Fourier transform of  $V_i(r)$  is

$$V_{i}(k) = (-4\pi Z_{i}e^{2}/\Omega k^{2}) \left[ (1 - \alpha_{i}) \cos kR_{m}^{i} + (\alpha_{i}/R_{m}^{i}) \left( \sin kR_{m}^{i}/k \right) \right], \tag{2}$$

where  $\alpha_1 \equiv V_1 R_m^{-1}/Z_1 e^2$ .  $\alpha$  is a measure of the well depth relative to the electrostatic potential at  $R_m$ . Its value varies according to the particular model used for the local potential, e.g.,  $\alpha = 0$  for the Ashcroft "empty-core" potential and  $\alpha = 1$  for Shaw's optimized model potential. In the present work  $\alpha$  was fitted to give agreement with the elastic constants of aluminum.

On the basis of this expression for  $V_i(k)$ , one may discuss the effect of valence and ionic size on the interatomic potential. The factor in the brackets depends only on the parameters  $\alpha$  and  $R_m$ , and the other factor depends only on the ionic charge. One can consider these factors to describe respectively the "size" and valence effects on the interatomic potential. Substituting Eq. (2) into Eq. (1) one observes that  $\phi_{ab}(r)$  simply scales with the valence of the impurity. Changes in the impurity size may be simulated by changes in the model radius  $R_m^{-1}$  while the parameter  $\alpha$  is kept the same as that of the host atom. The size factor, as defined by  $R_m^{-1}$  in our model, is incorporated into the bare ion model potential. Since the interatomic potential is obtained by screening the bare ion potential, the effect of the impurity size depends also on the extent of the dielectric screening. This places the size effect in

387

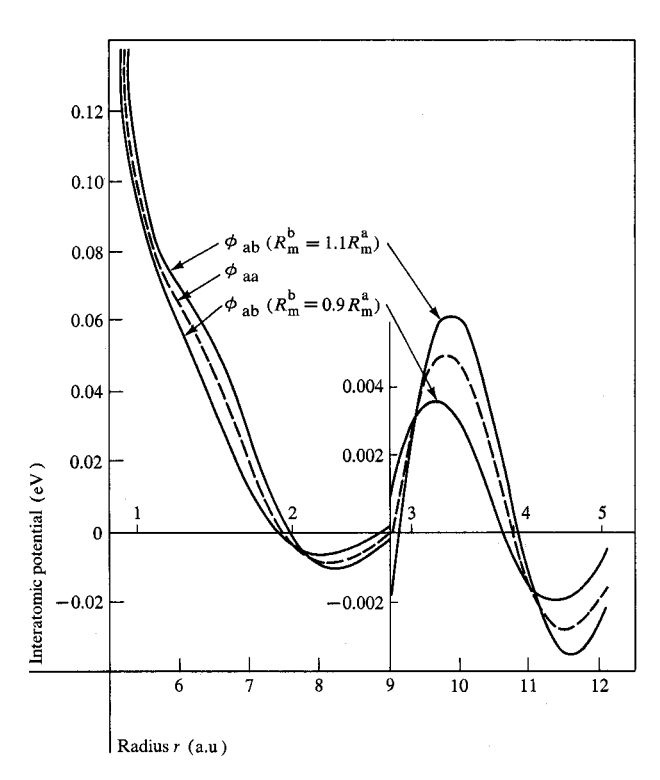


Figure 1 Interatomic potentials for homovalent impurities in Al. The potential scale has been expanded tenfold for r > 9 a.u. to show the oscillations in the potential. The positions of the first five neighbors are also indicated. The parameters used in the host potential are  $R_{\rm m}^{\ a} = 0.71$  Å and  $\alpha_{\rm a} = 0.42$ .

a framework quite different from some of the earlier models [12] that treat primarily the elastic interaction between the defects.

In general, of course,  $\alpha$  may also vary. However, appropriate values of the parameters  $\alpha$  and  $R_{\rm m}$  for specific impurities are not presently known. Therefore we attempt to ascertain in a general way the effects of size and valence of the impurity on diffusion without specifying explicitly the impurity that is being considered.

 $\phi_{ab}(r)$  for impurities with model radius 10 percent larger and smaller than the host, along with  $\phi_{aa}(r)$  for aluminum, is shown in Fig. 1. The impurity potentials are seen to have forms similar to that of the host-host potential and exhibit oscillations starting at the third-neighbor position. In the present calculations, the potentials are truncated at the fifth-neighbor position. The exact form of the potential is extremely sensitive to the particular dielectric function used, as recently emphasized by Duesbery and Taylor [13]. The importance of the dielectric screening is underlined by the fact that even at the first-neighbor position the effective interaction  $\phi_{aa}(r)$  is reduced by 99.7 percent from the bare Coulomb interaction. The choice of the dielectric function is therefore critical for the construction of the interatomic poten-

tial. In the present work, the dielectric function of Geldart and Taylor [14] has been employed. These authors have computed electron gas exchange and correlation contributions in such a way that the important compressibility sum rule is satisfied. Our pseudopotential parameters for aluminum,  $R_{\rm m}=0.71$  Å and  $\alpha=0.42$ , have been determined by fitting to the measured elastic constants. Phonon dispersion curves and vacancy formation and migration energies calculated on the basis of this pseudopotential are in good agreement with experimental values.

In comparing the potentials in Fig. 1, one observes a systematic change in the amplitude and phase of the oscillation as a function of the model radius. The potential for the smaller ion has weaker oscillations and a more advanced phase. This reflects a more complete screening of a smaller ion than a larger one. The overall difference in the magnitudes of the potentials is quite small, which again results from the completeness of the dielectric screening.

#### Relaxation calculation

In the calculation of lattice relaxation and relaxation energies, the Green's function formulation of lattice statics [1] was employed. In this approach, certain lattice dynamical techniques are applied in the zero-frequency limit to obtain the static equilibrium configuration of atoms around a point defect. A brief outline of the Green's function method and how it applies to the particular defect configurations of interest in this work is given in this section.

As in the harmonic approximation of lattice dynamics one expands the crystal energy to second order in the atomic displacements:

$$\Phi = \Phi_0 - \sum_{l,\alpha} F_{\alpha}(l) u_{\alpha}(l) + \frac{1}{2} \sum_{\substack{l' \\ l' \\ \beta}} \phi_{\alpha\beta}(l,l') u_{\alpha}(l) u_{\beta}(l'). \tag{3}$$

Here  $u_{\alpha}(l)=r_{\alpha}(l)-R_{\alpha}(l)$  is the displacement of atom l from its unrelaxed position (i.e., a perfect lattice site unless l corresponds to an interstitial). The coefficients  $F_{\alpha}(l)$  and  $\phi_{\alpha\beta}(l,l')$  are determined from the interatomic potentials.

The equilibrium condition  $\partial \Phi / \partial u_{\alpha}(l) = 0$  may be expressed in matrix form as  $\phi u = F$ , or

$$u = \phi^{-1} F \equiv GF. \tag{4}$$

The central problem in this approach is that of inverting  $\phi$  to obtain the Green's function G.

Any point defect may be considered to be some combination of  $n_v$  vacancies and  $n_i$  interstitials. We refer to each particular case by the shorthand notation  $(n_v, n_i)$ . For example: vacancy, (1, 0); interstitial, (0, 1); "activated" or migrating vacancy, (2, 1); etc. The  $n_v$  vacancies and  $n_i$  interstitials comprise the defect "core."

It is convenient to divide  $\phi$  into two parts,

$$\phi = \phi^0 - \delta\phi, \tag{5}$$

where  $-\delta \phi$  is essentially the change in  $\phi$  caused by the introduction of the defect. The matrix  $\phi$  and the vectors u and F in Eq. (4) are of dimension  $D = 3(N + n_i)$  where N is the total number of lattice sites. The matrix  $\phi^0$  takes account only of the interactions present in the perfect crystal.  $-\delta \phi$  is the change in  $\phi$  which occurs upon "turning on" the interactions of the  $n_i$  interstitial atoms and "turning off" the interactions corresponding to the  $n_{ij}$ vacant sites. This procedure for splitting  $\phi$  is illustrated schematically in Fig. 2 for the case of an impurity at the saddle point, i.e., (2, 1). For simplicity, only the (111) plane with nearest-neighbor interactions is shown. In the calculation of  $\phi^0$  the interstitial atoms are treated as noninteracting free particles.  $-\delta\phi$  accounts for the interactions of the impurity atom and the "turning off" of the interactions for the vacant site at the origin.

The substitution of Eq. (5) into Eq. (4) yields

$$G = (1 - G^{0}\delta\phi)^{-1}G^{0} = G^{0} + G^{0}\delta\phi G, \tag{6}$$

where  $G^0 \equiv (\phi^0)^{-1}$ 

Equation (6) is the familiar Dyson equation for Green's function. The methods for solving this equation are described in detail by Tewary [1] and therefore are only discussed in general terms here. Two features simplify the analysis. First, the assumption of finite range interatomic interactions implies that only a small number of the coefficients  $F_{\alpha}(l)$  and  $\delta\phi_{\alpha\beta}(l,l')$  are nonzero (in the present calculations we consider interactions extending to fifth nearest neighbors). By applying the procedure of matrix partitioning [15] to Eq. (4) one obtains the relation

$$u_{p} = gf, (7)$$

where

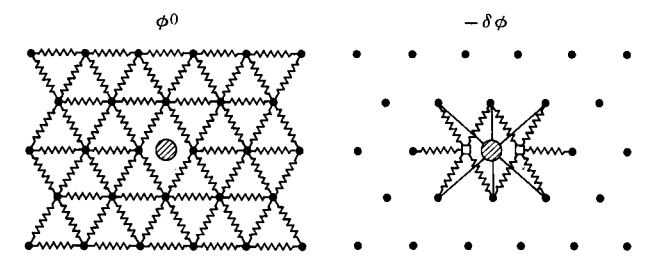
$$g = g^0 + g^0 \delta \phi_n g.$$

Equation (7) governs the displacements of atoms in the "perturbed space," which consists of the defect core plus the  $n_c$  lattice atoms that interact directly with the core. (For the configuration shown in Fig. 2,  $n_c = 116$ ). The matrices g,  $g^0$  and  $\delta \phi_p$  and the vectors  $u_p$  and f are of dimensions  $3n_p$ , where  $n_p = n_i + n_v + n_c$ .

After g has been determined, displacements of atoms outside the perturbed space may also be calculated [15]. However, this is not necessary if one is interested only in the relaxation energy. Substituting Eq. (4) into Eq. (3), one may express the relaxation energy as

$$E_{\rm R} = \phi - \phi_0 = -Fu + \frac{1}{2}u\phi u = -\frac{1}{2}Fu = -\frac{1}{2}fu_{\rm p}.$$
 (8)

The second simplifying feature derives from the symmetry of the lattice relaxation field. Some of the atomic



- Host atom
- □ Vacancy

**Figure 2** Schematic illustration of splitting  $\phi$  into  $\phi^0$  and  $-\delta\phi$  for the saddle-point configuration of an impurity  $\omega_0$  jump.

displacements  $u_{\alpha}(l)$  are equal to others by virtue of this symmetry, and therefore the number of degrees of freedom in the perturbed space is less than  $3n_{\rm p}$ . This allows one to obtain a "reduced" version of Eq. (7):

$$u^{r} = g^{r} f^{r}. (9)$$

Here the reduced vectors and matrices are defined by the relations

$$u_i^{\,\mathrm{r}} = \sum_{l\alpha} \psi_\alpha^{\,i}(l) \ u_\alpha(l), \tag{9a}$$

$$f_i^{\mathsf{r}} = \sum_{l} \psi_{\alpha}^{\;i}(l) f_{\alpha}(l), \tag{9b}$$

$$g_{ij}^{\ r} = \sum_{ll'} \psi_{\alpha}^{\ i}(l) \ g_{\alpha\beta}(l, l') \ \psi_{\beta}^{\ j}(l'),$$
 (9c)

where the  $\psi^i$  are "basis" vectors in the perturbed space. The number of distinct basis vectors having the proper symmetry is equal to  $n_r$ , the number of degrees of freedom in the perturbed space. The perturbed space displacements are related to the  $u_i^{\ r}$  by the inversion formula

$$u_{\alpha}(l) = \sum_{i}^{n_{\mathbf{r}}} \psi_{\alpha}^{i}(l) \ u_{i}^{\mathbf{r}}. \tag{10}$$

The reduced Green's function is determined from the Dyson equation

$$g^{r} = [(1 - g^{0} \delta \phi)^{r}]^{-1} g^{0r} \equiv (A^{r})^{-1} g^{0r}. \tag{11}$$

Equation (8), in conjunction with Eqs. (9)-(11), provides a means for calculating relaxation energies. The defect configurations for which we require relaxation energies are illustrated in Figs. 3 and 5 and are discussed in detail in the fourth and fifth sections. We point out here that for each configuration the defect core may be found by inspection. Migrating atoms at saddle point sites and impurity atoms are treated formally as interstitials [16]. A substitutional impurity is treated as an interstitial superimposed on a vacancy. For example, substitutional impurity atom, (1, 1); migrating impurity atom ( $\omega_2$  jump),

389

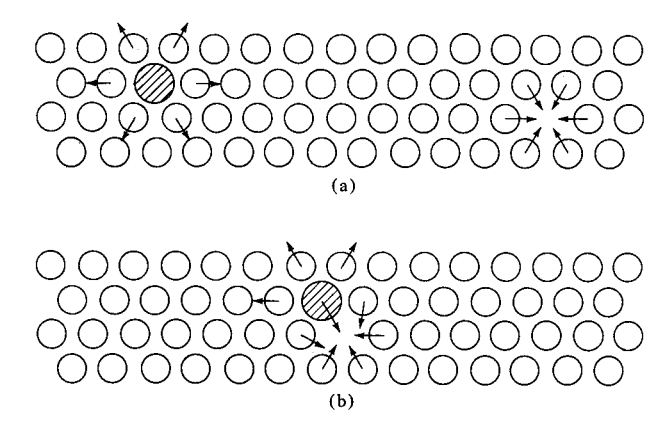


Figure 3 The formation of an impurity-vacancy pair in (b) is accomplished by bringing together the isolated vacancy and impurity in (a).

(2, 1); dissociative jump configuration ( $\omega_3$  jump), (3, 2); etc. After the defect core for a particular configuration is identified and the appropriate interatomic potentials are specified, the calculation of the relaxation energy may proceed as we have outlined in this section.

Finally, some technical details should be mentioned here. The dimension  $3n_p$  of the perturbed space is typically large enough that direct multiplication to obtain the product  $g^0\delta\phi$  in Eq. (11) is quite time-consuming even when performed on a computer. It is somewhat more convenient to compute the matrix  $A^r$  from the relation

$$A^{r} = \widetilde{A}^{r} + \delta A^{r}, \tag{12}$$

where

$$\widetilde{A}^{r} = 1 - g^{0r} \delta \phi^{r}, \tag{12a}$$

$$\delta A_{ij}^{r} = -\sum_{l\alpha} \sum_{l'\alpha'l''\beta} \psi_{\alpha}^{i}(l) g_{\alpha\beta}^{0}(l, l'') \times \delta \phi_{\beta\alpha'}(l'', l) \psi_{\alpha'}^{i}(l').$$
(12b)

The reduced matrices  $g^{0r}$  and  $\delta \phi^r$  are defined in analogy to  $g^r$  in Eq. (9c). In Eq. (12b) the l' sum includes the  $n_v$  core vacancies. The basis vectors  $\psi$  possess no nonzero elements in the space of the core vacancies. Therefore, the contribution to  $A^r$  due to these vacancies is accounted for explicitly in the term  $\delta A^r$ . In the case of a monovacancy or a substitutional impurity, it is easy to show that  $\delta A^r = 0$  as a consequence of the inversion symmetry about the defect site. For more complicated configurations  $\delta A^r$  is in general nonzero and must be accounted for.

In the lattice statics calculations performed in this work, pairs of atoms were assumed to interact via central forces. In this model, the  $\phi$  matrix may be expressed in terms of the first two derivatives of the interatomic potential:

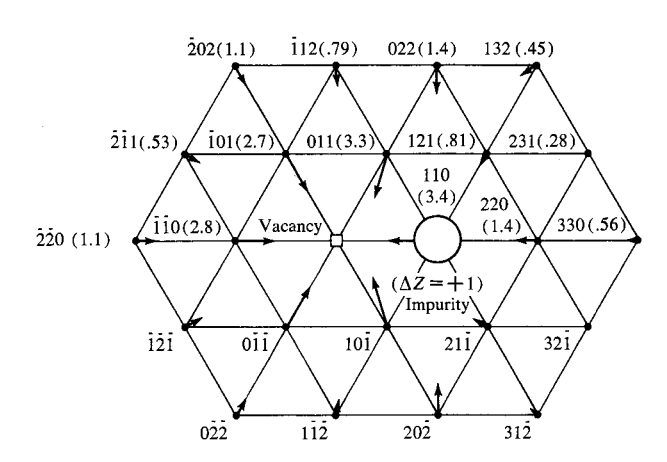


Figure 4 (111) projection of displacement field for vacancy-impurity pair in Al. This impurity has  $Z_b = 4$  but the same  $R_m$  as Al.

$$\begin{split} \phi_{\alpha\beta}(l,\,l') &= \left( -\,\delta_{\alpha\beta} + \frac{\mathbf{r}_{\alpha}\mathbf{r}_{\beta}}{r^2} \right) \frac{1}{r} \frac{d\phi(r)}{dr} \\ &\quad - \frac{\mathbf{r}_{\alpha}\mathbf{r}_{\beta}}{r^2} \frac{d^2\phi(r)}{dr^2}, \qquad l' \neq l; \\ \phi_{\alpha\beta}(l,\,l) &= -\sum_{l' \neq l} \phi_{\alpha\beta}(l,\,l'), \end{split}$$

where  $r = \mathbf{R}(l) - \mathbf{R}(l')$  and  $\phi(r)$  is the interatomic potential connecting atoms l and l'.

## Impurity-vacancy binding energy

Figure 3(b) illustrates a vacancy-impurity pair in the nearest-neighbor configuration, and Fig. 3(a) shows such a pair separated by a large distance. The binding energy  $E_{\rm b}$  is the difference [17] in the crystal energies for these two configurations. In the appendix we show that this difference may be expressed in terms of pair interactions alone. It is convenient to divide the binding energy into two parts; one, which we call  $E_{\rm b}^{\rm c}$ , corresponds to the unrelaxed lattices, while the other,  $E_{\rm b}^{\rm R}$ , accounts for the lattice relaxation. With reference to Figs. 3(a) and 3(b), the "configuration" energy  $E_{\rm b}^{\rm c}$  may be written immediately as

$$E_{\rm b}^{\ c} = \phi_{\rm AB}(r_1) - \phi_{\rm AA}(r_1),$$

where  $r_1$  is the nearest-neighbor distance. The calculation of  $E_b^{\ R}$  is more involved since it requires the application of the lattice statics method described in the previous section to obtain the relaxation energies for the vacancy-solute pair, the isolated vacancy, and the substitutional impurity. If these energies are called, respectively,  $E_R^{\ vs}$ ,  $E_R^{\ v}$  and  $E_R^{\ s}$ , one may write  $E_b^{\ R} = E_R^{\ s} + E_R^{\ v} - E_R^{\ vs}$ . The calculation of the first two terms is relatively easy, since  $n_r = 7$ , and  $\delta A^r = 0$ . The calculation of  $E_R^{\ vs}$  is more dif-

ficult, however, since  $n_r = 96$  and  $\delta A^r \neq 0$ . A useful self-consistency check on the latter calculation is available. If the solute is treated as simply another host atom in the impurity-vacancy pair calculation, one should obtain results identical to those for the isolated vacancy. This was in fact verified in our calculations.

In Fig. 4 is illustrated the displacement field in a (111) plane containing a vacancy-impurity pair, for an impurity of valence 4. As required, the displacements exhibit axial symmetry about the vacancy-impurity line. The magnitudes of the individual atomic displacements reflect the extra attraction associated with the impurity; compare, for example, the 2.8 percent inward displacement of the  $\bar{1}\bar{1}0$  atom with the 3.4 percent displacement of the impurity.

In Table 1, the results of the binding energy calculation are given. For impurities that differ only in valence from the host, the binding energy results primarily from  $E_b^{\ c}$ . However, the relaxation energy  $E_b^{\ R}$  is not negligible and it always reduces  $E_b$ . The sign of  $E_b$  depends on the sign and magnitude of  $\phi_{AA}(r_1)$ , which in turn depends on the dielectric screening. In the present case, since  $\phi_{AA}(r_1)$  is positive, a divalent impurity is repelled by the vacancy and a negative  $E_b$  is expected. The opposite situation exists for a quadrivalent impurity. For impurities differing only in size from the host,  $E_b^{\ R}$  is quite important relative to  $E_b^{\ c}$ , as one can see from the results in Table 1. The sign of  $E_b$  for such impurities depends on the balance of  $E_b^{\ c}$  and  $E_b^{\ R}$ .

Overall, the binding energies are quite small. It is possible to obtain an upper bound for the binding energy of impurities by setting  $E_b^c$  equal to  $\phi_{AA}(r_1)$  and ignoring the contribution from the relaxation energy. Based on the effective potential for Al in Fig. 1, this upper limit is estimated to be 0.1 eV. This value, of course, depends on the dielectric function used in calculating the potential. However, judging from the magnitude of other Al po-

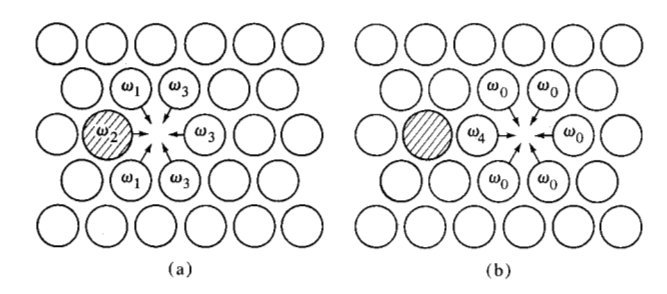


Figure 5 Various atomic jump frequencies entering kinetic analysis of impurity diffusion in the Howard-Manning [19] model.

tentials, e.g., those derived by Duesbery and Taylor [13] and Shyu et al. [18], the value of 0.1 eV appears to be a valid estimate.

## Activation energy for impurity diffusion

The kinetics for impurity diffusion in an fcc lattice has been studied by Howard and Manning [19]. Figures 5(a) and 5(b) depict the various atomic jumps entering their model. The ratio of the diffusivities of the impurity and the host atom can be expressed as [19]

$$D_{\rm b}/D_{\rm a} = (f_{\rm b}/f_{\rm a})(\omega_2/\omega_0)(\omega_4/\omega_3),$$

where the first term is the ratio of the correlation factors, the second term the ratio of the frequencies of the saddle-point jumps for the impurity and the host, and the last term the ratio of the associative and dissociative jump frequencies for the vacancy-impurity pair. The second term is related to the migration energy difference and the third to the binding energy. One can write the difference in the diffusion activation energies as [20]

$$\Delta Q = \Delta E - E_{\rm b} - k \, \partial \ln f_{\rm b} / \partial (1/T), \tag{13}$$

where  $\Delta E$  is the difference in migration energies for the impurity and the host atom, and the last term arises from

Table 1 Theoretical binding energy for impurity-vacancy pair in aluminum (all units in eV).

Impurity	$\phi_{ab}(r_1)$	$E_{ m b}^{\  m c}$	$E_{\mathrm{R}}^{-\mathrm{s}}$	$E_{ m R}^{\  m vs}$	$E_{ m b}^{\  m R}$	$E_{\mathrm{b}}$
$Z_{\rm b}=2$	0.069	-0.034	-0.008	-0.104	0.012	-0.022
$R_{\rm m}^{\ \ \rm b} = R_{\rm m}^{\ \ \rm a}$						
$Z_{\rm b} = 4$	0.138	0.035	0.007	-0.075	-0.016	0.019
$R_{\rm m}^{\ \ \rm b} = R_{\rm m}^{\ \ \rm a}$						
$Z_{\rm b}=3$	0.099	-0.004	-0.002	-0.091	0.005	0.001
$R_{\rm m}^{\ \ b} = 0.9 R_{\rm m}^{\ \ a}$						
$Z_{\rm b}=3$	0.115	0.012	-0.005	-0.075	-0.014	-0.002
$R_{\rm m}^{\rm b} = 1.1 R_{\rm m}^{\rm a}$						

Note:  $\phi_{AA}(r_1) = 0.103$ ;  $E_R^{\ v} = -0.084$ 

**Table 2** Theoretical  $\Delta E$  for impurity migration in aluminum (all units in eV).

Impurity	$E_{\mathrm{C}}^{\mathrm{s}}\left(\omega_{2}\right)$	$\Delta E_{ m c}$	$E_{\mathrm{R}}^{\mathrm{s}}\left(\omega_{2}\right)$	$\Delta E_{ m R}$	$\Delta E$
$Z_{\rm b} = 2$	1.318	-0.276	-0.243	0.209	-0.067
$R_{\rm m}^{\ b} = R_{\rm m}^{\ a}$ $Z_{\rm b} = 4$	2.637	0.276	-0.648	-0.225	0.051
$R_{\rm m}^{\ b} = R_{\rm m}^{\ a}$ $Z_{\rm b} = 3$	1.619	-0.306	-0.279	0.160	-0.146
$R_{\rm m}^{\rm b} = 0.9 R_{\rm m}^{\rm a}$ $Z_{\rm b} = 3$ $R_{\rm m}^{\rm b} = 1.1 R_{\rm m}^{\rm a}$	2.449	0.347	-0.643	-0.220	0.127

Note:  $E_{\rm c}^{\ \ s}(\omega_{\rm p})$  is the "configuration" energy for the unrelaxed impurity saddle-point. Other parameters needed for calculating  $\Delta E$  are: 1.977 eV for the configuration energy of the host saddle-point and -0.432 eV for  $E_{\rm R}(\omega_{\rm p})$ .

Figure 6 Valence of  $R_{\rm m}$  for various elements obtained by Shaw [9] for the optimized model potential vs Pauling ionic radii [25]. Diffusion data for impurity in Al are given in the table below. The references for these data are given in the second part of [2].

Solute	$Valence\ charge\ of\ solute\ (Z_{ m s})$	$egin{aligned} E_{\mathfrak{b}} \ (\mathbf{eV}) \end{aligned}$	$rac{\Delta Q}{({ m eV})}$
Cu	1	0.00	0.14
Ag	1	0.05	-0.05
Ag Zn	2	0.02	-0.006
Cd	2		0.03
Ga	3	≤0.04	0.01
In	3	_	0.01

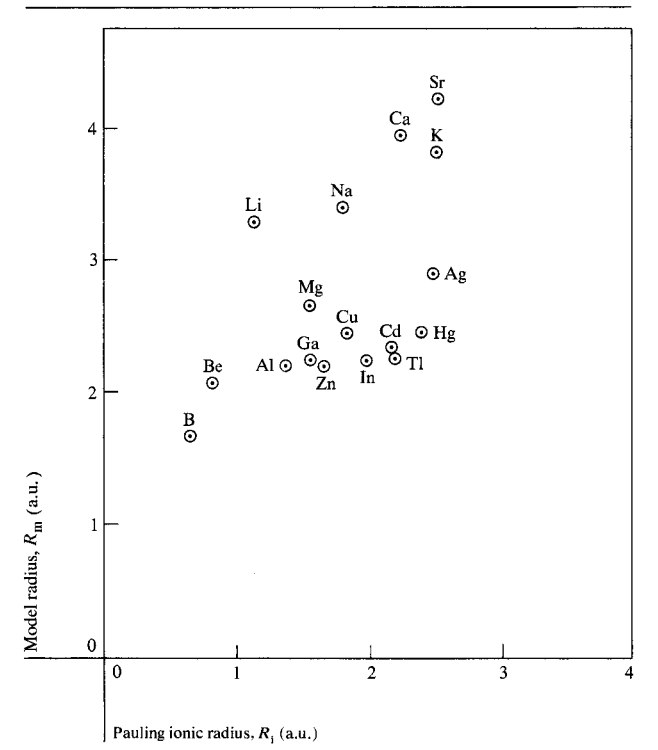


**Table 3** Theoretical  $\Delta Q$  for impurity diffusion in aluminum (all units in eV).

Impurity	$\Delta E$	$E_{\mathrm{b}}$	$\Delta Q$
$Z_{\rm b} = 2$	-0.067	-0.022	-0.045
$R_{\rm m}^{\rm b} = R_{\rm m}^{\rm a}$ $Z_{\rm b} = 4$	0.051	0.019	0.032
$R_{\rm m}^{\rm b} = R_{\rm m}^{\rm a}$ $Z_{\rm b} = 3$	-0.146	0.001	-0.145
$R_{\rm m}^{\rm b} = 0.9 R_{\rm m}^{\rm a}$ $Z_{\rm b} = 3$	0.127	-0.002	0.125
$R_{\rm m}^{\rm b} = 1.1 R_{\rm m}^{\rm a}$			

the temperature dependence of the correlation factor for the impurity. The last term can be calculated from the temperature dependence of the jump frequencies in the kinetic model. Peterson and Rothman [5] estimated it to be very close to zero for monovalent and divalent impurities in Al, independent of whether the electrostatic model or the oscillatory potential is used. These authors also reported a preliminary measurement of this term for Zn isotopes and found a small value of less than 0.1 eV. For simplicity, we assume this term to be zero here.

In analogy to our treatment of the impurity binding energy,  $\Delta E$  may be divided into a "configuration" contribution  $\Delta E_{\rm c}$  associated with the unrelaxed saddle-point configurations and a contribution  $\Delta E_{\rm R}$  resulting from lattice relaxation. In calculating  $\Delta E_{\rm c}$  or  $\Delta E_{\rm R}$ , one has to account not only for the different saddle-point configurations but also the different initial lattices. Thus

$$\Delta E_{\rm R} = [E_{\rm R}^{\ \ s} \ (\omega_{\rm 2}) - E_{\rm R}^{\ \ vs}] - [E_{\rm R}(\omega_{\rm 0}) - E_{\rm R}^{\ \ v}],$$

where the relaxation energies are associated respectively with the impurity saddle point, impurity-vacancy pair, host-atom saddle point and isolated vacancy. A similar expression exists for  $\Delta E_{\rm c}$ .

In Table 2, numerical values calculated for  $\Delta E$  are presented. It is found that the value of  $\Delta E_{\rm c}$  is determined mainly by the sign and magnitude of  $\phi_{\rm AA}$  at the distance from the saddle-point to one of the four "ring" lattice sites. In the present calculation,  $\phi_{\rm AA}$  at that distance is positive; therefore, a divalent impurity interacts less strongly with its surrounding atoms than a host atom because of its smaller valence. This gives rise to a negative  $\Delta E_{\rm c}$ . A similar situation exists for the homovalent impurity with model radius smaller than the host. The contribution from relaxation energies is observed to be comparable to that from  $\Delta E_{\rm c}$  and therefore must be carefully calculated to ensure a reliable value for  $\Delta E$ .

Table 3 gives results for  $\Delta Q$ , neglecting the final term in Eq. (13). Comparing the values of  $\Delta E$  and  $E_{\rm b}$ , one observes that the size and valence have a larger effect on impurity migration than on binding energies.

#### Discussion

It is interesting to compare the present results with available data on the binding energy and activation energy for nontransition-metal impurities in Al. In doing so, it is important to keep in mind that, since our calculations do not specify particular impurities, the comparison is only semiquantitative. Furthermore, it is difficult to extrapolate our results to very different impurity parameters. In a recent review by Balluffi and Ho [2], it was noted that the equilibrium experiments, such as the lattice expansion and positron annihilation measurements, give binding energies consistently lower than those obtained from quenching-annealing experiments. Our results seem to support the smaller binding energies obtained from the equilibrium measurements. For some impurities, the agreement is even quantitative; for example, Si has a valence of 4 and an  $E_b$  of 0.03 eV [21], and Mg is divalent and its  $E_{\rm b}$  was measured to be -0.1 ±0.04 eV [22], or <0.05 eV [23].

In Fig. 6 we list experimental values of  $\Delta O$  for three solute pairs (Cu, Ag), (Zn, Cd) and (Ga, In) together with values of  $R_{\rm m}$  for various elements recently determined by Shaw [9, 24]. In view of their model radii, the homovalent pair (Ga, In) should be almost equal in size to Al, and therefore their  $\Delta Q$  values are expected to be quite small. This prediction is consistent with the experimental results. For the divalent pair (Zn, Cd), the valence effect is expected to dominate in Zn, because its  $R_m$ is nearly equal to that of Al; on this basis a negative  $\Delta Q$ is predicted. For Cd, which is larger than Zn, the size effect is expected to compensate the valence effect. These predictions appear to be in accord with experimental data;  $\Delta Q$  for Cd is larger than for Zn and has the opposite sign. However, our calculated  $\Delta Q$ 's appear to exceed the measured values. The same line of reasoning fails when applied to the monovalent noble metal pair (Cu, Ag). Ag is larger than Cu and is therefore expected to have a higher  $\Delta Q$ , but this is not borne out by experimental observation. Thus, our calculation does not seem to account even qualitatively for the behavior of noble metal impurities. This is not surprising because the applicability of a simple model potential to d-band metals is questionable.

In the foregoing discussion, we have taken the model radius  $R_{\rm m}$  rather than, say, the Pauling ionic radius  $R_{\rm i}$  (cf. Fig. 6) to represent the impurity "size." The former parameter is a characteristic of the metallic state and is therefore more appropriate in the present context. One may note in Fig. 6 that in certain cases a large discrepancy exists between  $R_{\rm m}$  and  $R_{\rm i}$ . For example, the series

of trivalent elements Al, Ga, In and Tl have almost equal model radii but their ionic radii vary by almost a factor of two

In view of model radii plotted in Fig. 6, the monovalent pair Na and K and the divalent pair Be and Mg appear to be interesting elements for experimental study. All of these can be classified as typical simple metal ions and the model radii of the two members of each pair are quite different. At present, there are no reliable diffusion data for these impurities in aluminum.

Finally, we consider the validity of the almost universally adopted nearest-neighbor model for the kinetic analysis of impurity diffusion in fcc crystals. A crucial question is whether the binding energy for a vacancy-impurity pair beyond the nearest-neighbor distance is negligible compared to that for a nearest-neighbor pair. To settle this point, further detailed calculation of the binding energy would be required. However, judging from the generally small values obtained here for the binding energy of a nearest-neighbor pair, it seems possible that some more distant pairs can have comparable stability. If this were the case, a kinetic model incorporating more distant jumps than those shown in Fig. 5 would be required. For Al, values of the interatomic potential from the second- to the fifth-neighbor positions are comparable in magnitude and therefore any extension beyond the nearest-neighbor model would be very complicated.

#### **Acknowledgment**

One of us (R.B.) acknowledges the support provided by the United States Atomic Energy Commission under contract AT (11-1)-3158.

#### **Appendix**

It is shown here that the volume-dependent part of the crystal energy may be neglected in binding energy and migration energy calculations.

Consider the migration of an isolated vacancy. The migration energy may be expressed as

$$E_{\rm m} = \Phi_{\rm sp}(N, \Omega_{\rm sp}) - \Phi_{\rm v}(N, \Omega_{\rm v}), \tag{A1}$$

which is the difference in crystal energies for the saddle point and simple vacancy configurations. N is the number of atoms and  $\Omega$  the total volume of the relaxed crystal. Because the vacancy formation volume differs in general from the self-diffusion activation volume,  $\Omega_{\rm sp} \neq \Omega_{\rm v}$ . Subtracting and adding the energy of a perfect crystal,  $\Phi(N,\Omega)$ , to Eq. (A1), one obtains

$$\begin{split} E_{\rm m} &= \left[ \Phi_{\rm sp}(N,\,\Omega_{\rm sp}) - \Phi(N,\,\Omega) \right] - \left[ \Phi_{\rm v}(N,\,\Omega_{\rm v}) \right. \\ &\left. - \Phi(N,\,\Omega) \right] \equiv E_{\rm f}^{\rm sp} - E_{\rm f}^{\rm v}. \end{split} \tag{A2}$$

The term within the second pair of brackets is simply the vacancy formation energy. In earlier work [15], it was shown that this may be expressed in the form

393

$$E_{\rm f}^{\rm v} = E_{\rm c}^{\rm v} + E_{\rm R}^{\rm v} - E_{\rm d} - E_{\rm s},$$
 (A3)

where the first two terms on the right-hand side are, respectively, the "configuration" and "relaxation" energies,  $E_{\rm d}$  is the change in pairwise interaction energy associated with a uniform expansion of the crystal by one atomic volume, and  $E_{\rm s}$  is the pairwise interaction energy of a surface atom. In deriving Eq. (A3), the perfect crystal is taken to be at equilibrium. An expression similar to (A3) may be derived for  $E_{\rm r}^{\rm sp}$ ,

$$E_{\rm f}^{\rm sp} = E_{\rm c}^{\rm sp} + E_{\rm R}^{\rm sp} - E_{\rm d} - E_{\rm s}.$$
 (A4)

Substituting Eq. (A4) and (A3) into (A2), one obtains

$$E_{\rm m} = E_{\rm m}^{\rm c} + E_{\rm m}^{\rm R},$$

where

$$E_{\rm m}^{\rm c} = E_{\rm c}^{\rm sp} - E_{\rm c}^{\rm v},$$

$$E_{\rm m}^{\rm R} = E_{\rm R}^{\rm sp} - E_{\rm R}^{\rm v}.$$

The migration energy is thus expressed in terms of configuration and relaxation contribution, both of which are determined by the pairwise interactions.

The above discussion is concerned with the migration of an isolated vacancy. Similar derivations may be carried out for the impurity-vacancy binding energy and migration energies in the presence of an impurity. One obtains, for example,

$$E_{\rm b} = E_{\rm b}^{\ c} + E_{\rm b}^{\ R},$$

a relation used in our section on impurity-vacancy binding energy.

#### References and notes

- V. K. Tewary, A.E.R.E. Harwell Report T.P. 548, 1973; see also R. Benedek and P. S. Ho, J. Phys. F: Metal Phys. 3, 1285 (1973).
- N. H. March and J. S. Rousseau, Crystal Lattice Defects
   1 (1971); R. W. Balluffi and P. S. Ho, ASM Seminar for Diffusion, ed; H. I. Aaronson (American Society of Metals, Cleveland, Ohio, 1974).
- D. Lazarus, Phys. Rev. 93, 973 (1954); L. C. R. Alfred and N. H. March, Phil Mag. 2, 985 (1957); A. D. LeClaire, Phil. Mag. 7, 141 (1962).
- A. Blandin, J. L. Deplante and J. Friedel, Proc. Kyoto Conf. on Crystal Lattice Defects, J. Phys. Soc. Japan 18, Suppl. II, 85 (1963).

- N. L. Peterson and S. J. Rothman, Phys. Rev. B 1, 3264 (1970).
- V. Heine and D. Weaire in Solid State Physics, vol. 24, eds;
   H. Ehrenreich et al., Academic Press, New York, 1970.
- 7. See for example: W. A. Harrison, *Pseudopotentials in the Theory of Metals*, Benjamin Inc., New York, 1966.
- 8. N. W. Ashcroft, in *Interatomic Potentials and Simulation of Lattice Defects*, eds., P. C. Gehlen, et al., Plenum Press, New York, 1972, pp. 91-110.
- 9. R. W. Shaw, Jr., Phys. Rev. B 5, 4742 (1972).
- P. S. Ho, Phys. Rev. B 3, 4035 (1971); ibid., 7, 3550 (1973).
- 11. V. Heine and I. Abarenkov, Phil. Mag. 9, 451 (1964).
- D. Lazarus, Phys. Rev. 93, 973 (1954) and R. A. Swalin, Acta Met. 5, 443 (1957).
- 13. M. S. Duesbery and R. Taylor, Phys. Rev. B 7, 2870 (1973).
- D. J. W. Geldart and R. Taylor, Can. J. Phys. 48, 167 (1970).
- R. Benedek and P. S. Ho, J. Phys. F; Met. Phys. 4, 181 (1974).
- 16. An impurity atom is treated formally as an interstitial even if it occupies a substitutional site, because its force constants differ from those of the host.
- 17. We adopt the usual sign convention for the binding energy; E<sub>b</sub> is positive if the crystal has lower total energy in the nearest-neighbor configuration.
- W. M. Shyu, J. H. Wehling, M. R. Cordes and G. D. Gaspari, *Phys. Rev. B* 4, 1802 (1971).
- R. E. Howard and J. R. Manning, Phys. Rev. 154, 561 (1967).
- 20. A. D. LeClaire, Phil. Mag. 7, 141 (1962).
- 21. J. Burke and A. D. King, Phil. Mag. 21, 7 (1970).
- D. R. Beaman, R. W. Balluffi and R. S. Simmons, *Phys. Rev. A* 137, 917 (1965).
- B. T. A. McKee, A. T. Stewart and M. J. Stott, Conf. on Point Defects and Their Aggregates in Metals, University of Sussex, England, 1972.
- 24. Shaw determined these  $R_{\rm m}$  values based on his optimized model potential which, in its local form, is equivalent to setting  $\alpha=1$ . As a result, his  $R_{\rm m}$  value for Al is considerably larger than ours.
- L. Pauling, The Nature of the Chemical Bond, Cornell University Press, Ithaca, New York, 1940.

Received February 6, 1974

Dr. Ho is located at the IBM Thomas J. Watson Research Center, Yorktown Heights, New York 10598. Dr. Benedek is located at the Department of Materials Science and Engineering, Cornell University. Ithaca, New York 14850.